DOI: 10.1002/ejic.200600711

Coordinative Versatility of Guanazole [3,5-Diamino-1,2,4-triazole]: Synthesis, Crystal Structure, EPR, and Magnetic Properties of a Dinuclear and a Linear Trinuclear Copper(II) Complex Containing Small Bridges and Triazole Ligands

Elena Aznar,[a] Sacramento Ferrer,*[a] Joaquín Borrás,[a] Francesc Lloret,[a] Malva Liu-González,[b] Héctor Rodríguez-Prieto,[c] and Santiago García-Granda[c]

Keywords: Copper / 1,2,4-Triazole ligands / Polynuclear compounds / X-ray structures / Magnetic properties

New complexes with guanazole (3,5-diamino-1,2,4-triazole = Hdatrz), $[Cu_2(Hdatrz)_2(\mu\text{-}OH_2)(H_2O)_4(SO_4)](SO_4)\cdot 3.5H_2O$ (**1**) and $[Cu_3(Hdatrz)_4(\mu\text{-}Cl)_2(H_2O)_4(SO_4)_2]\cdot 11.4H_2O$ (**2**), have been prepared and structurally characterized. Complex **1** is a noncentrosymmetric dinuclear compound in which the copper(II) ions are bridged by two triazole ligands and one μ-OH_2 molecule, with a Cu(1)···Cu(2) distance of 3.4945(8) Å. The chromophores are $Cu(1)N_2O_2O'$ (square pyramidal), and $Cu(2)N_2O_2O'O''$ (octahedral). Complex **2** has a linear trinuclear copper(II) structure, with two crystallographically independent copper(II) atoms. Neighboring copper(II) ions are linked by two triazole ligands and one slightly asymmetric chlorido bridge. The intratrimeric Cu(1)···Cu(2) distance is 3.5602 (4) Å. Cu(2), the central copper, is coordinated to N_4Cl_2 (octahedral) while Cu(1), the terminal copper, is coordinated to N_2O_2ClO' (also octahedral). Magnetic susceptibility measurements (2–300 K) are in accordance with the dinuclear (**1**) and trinuclear (**2**) nature of these compounds. The best-fit parameters, obtained with the Hamiltonian $\mathbf{H} = -J\Sigma_{i<j}\mathbf{S}_i\mathbf{S}_j$, are as follows: $g = 2.10(1)$ and $J = -94.3(2)$ cm^{-1} for **1**; and $g_{central} = 2.12(1)$, $g_{peripheral} = 2.07(1)$, and $J = -89.9(3)$ cm^{-1} for **2**. Compound **1**, which has an unprecedented *folded* bridging $\{Cu(N\text{–}N)_2Cu\}$ system, exhibits a magnetic exchange comparable to that of related *planar* compounds. Comparison of the magneto-structural properties of **2** with those of analogous linear trinuclear compounds has made a first approach to the relative magnitude of the *J* value possible. The Q-band powder spectra, which were recorded in a range from 4 K to room temperature, are in agreement with the magnetic susceptibility measurements.

Introduction

A variety of coordination compounds with 3,5-disubstituted 1,2,4-triazoles as ligands coordinating to transition-metal ions have been reported.[1–3] The interesting magnetic properties of the coordination compounds of iron(II) and copper(II) with 1,2,4-triazole ligands have been investigated extensively; among these, polynuclear (1,2,4-triazole)-iron(II) compounds have been found to show spin-crossover behavior.[4–7] These ligands allow for two general bridging modes, one involving only triazole bridges and another also containing either small bridging anions, such as Cl^-, F^-, NCS^-, N_3^- or OH^-, or small bridging molecules such as H_2O.[1]

Even though guanazole (3,5-diamino-1,2,4-triazole = Hdatrz) (Figure 1) is a simple molecule and an inexpensive chemical, only nine X-ray structures of complexes of this triazole have been documented to date and, to the best of our knowledge, none with Cu^{II} have been reported thus far. There is a similar lack of publications concerning the related unsubstituted 1,2,4-triazole ligand. In the latter case, the scarcity of structures has been attributed in part to the fact that the ligand often immediately produces a microcrystalline, insoluble precipitate with transition-metal ions.[1] The structures described for guanazole include one mononuclear compound with Pt^{II};[8] two two-dimensional polymers: one with Cd^{II}[9] and one with Mn^{II};[10] two cyclic trinuclear compounds of Pd^{II};[11,12] and four linear trinuclear compounds with $[M_3\{(H)datrz\}_6L_6]$ (L = H_2O or

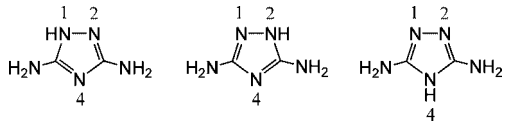

Figure 1. Tautomers of guanazole [Hdatrz].

[a] Departament de Química Inorgànica, Universitat de València, Vicent Andrés Estellés s/n, 46100 Burjassot, Valencia, Spain
E-mail: Sacramento.Ferrer@uv.es
[b] S.C.S.I.E. – Rayos X, Universitat de València, Vicent Andrés Estellés s/n, 46100 Burjassot, Valencia, Spain
[c] Departamento de Química Física y Analítica, Universidad de Oviedo, Julián Clavería 8, 33006 Oviedo, Spain

NCS^-) units: one with Co(II,III)[13] and three with Ni^{II}.[14–16] No dinuclear structures have been reported. It has been suggested that, because the substituents in position 3 and 5 are apparently capable of forming hydrogen bonds, the linking of metal ions by triple bridges is preferred.[1,17]

In the aforementioned structures, guanazole is known to coordinate in three different ways, either unidentate through *N*1, or bridging-bidentate through *N*1,*N*2 or *N*2,*N*4. Moreover, Hdatrz can occur in three different chemical forms, namely neutral (in most cases), anionic (with deprotonation at *N*4),[13] or cationic (with protonation at *N*2).[8] Especially interesting is the compound $[Co_3(datrz)_2(Hdatrz)_4(H_2O)_6]Cl_3{\cdot}9H_2O$, which includes mixed valences of cobalt ions and triazole/triazolate mixed ligand bridges.[13] Thus, in spite of its apparent simplicity, guanazole is quite a versatile ligand. As a result, we have found that the reaction solution often affords a mixture of compounds.

In this paper, we report on the isolation of two Cu^{II} compounds of Hdatrz with different nuclearity, one dinuclear (**1**) and the other linear trinuclear (**2**). Both compounds present double-triazole bridges and an additional small bridge, which is water in the case of **1** or chlorido in the case of **2**. Both compounds also contain the neutral *N*1,*N*2-bidentate ligand guanazole. We describe here the structural and spectroscopic characterization of these compounds, as well as the study of their magnetic properties in the context of related compounds.

Results and Discussion

Crystal Structure of $[Cu_2(Hdatrz)_2(\mu\text{-}OH_2)(H_2O)_4(SO_4)](SO_4){\cdot}3.5H_2O$ (1)

The structure of complex **1** is made up of dinuclear cations, one sulfate anion per cation, and non-coordinated water molecules, one of which is located on a symmetry site. There is one O(7) lattice water molecule per four Cu^{II} ions. An ORTEP view of the structure, together with its numbering scheme, is depicted in Figure 2. Selected bond lengths and angles are presented in Table 1.

Table 1. Selected bond lengths [Å] and bond angles [°] for **1**.

Cu(2)–N(1b)	2.005(4)	Cu(1)···Cu(2)	3.4945(8)
Cu(2)–N(2a)	1.986(5)	Cu(1)–N(2b)	1.988(3)
Cu(2)–O(1)	1.976(5)	Cu(1)–N(1a)	1.988(5)
Cu(2)–O(2)	2.000(4)	Cu(1)–O(3)	1.968(5)
Cu(2)–O(11)	2.425(4)	Cu(1)–O(4)	1.995(5)
Cu(2)–O(5)	2.382(5)	Cu(1)–O(5)	2.474(4)
O(5)–Cu(2)–N(1b)	81.8(2)	O(5)–Cu(1)–N(2b)	82.5(2)
O(5)–Cu(2)–N(2a)	90.0(2)	O(5)–Cu(1)–N(1a)	90.6(2)
O(5)–Cu(2)–O(11)	169.3(2)	O(5)–Cu(1)–O(3)	96.2(2)
O(5)–Cu(2)–O(1)	98.7(2)	O(5)–Cu(1)–O(4)	89.7(2)
O(5)–Cu(2)–O(2)	94.4(2)	N(1b)–Cu(2)–N(2a)	93.3(2)
Cu(1)–O(5)–Cu(2)	92.0(2)	N(2a)–Cu(2)–O(2)	87.2(2)
Cu(1)–N(1a)–N(2a)	119.9(3)	N(1b)–Cu(2)–O(1)	93.8(2)
Cu(1)–N(2b)–N(1b)	121.0(3)	O(11)–Cu(2)–O(1)	84.8(2)
Cu(2)–N(2a)–N(1a)	123.3(3)	O(11)–Cu(2)–O(2)	95.9(2)
Cu(2)–N(1b)–N(2b)	121.7(3)	O(11)–Cu(2)–N(2a)	87.7(2)
N(2b)–Cu(1)–N(1a)	91.4(2)	O(11)–Cu(2)–N(1b)	87.9(2)
N(2b)–Cu(1)–O(4)	89.1(2)	O(1)–Cu(2)–O(2)	86.3(2)
N(1a)–Cu(1)–O(3)	88.0(2)		
O(3)–Cu(1)–O(4)	91.4(2)		

In the dinuclear unit, the two copper centers, which are crystallographically independent, are bridged by two neutral guanazole ligands and one water molecule. The coordination environment around Cu(1) is distorted square pyramidal, with two triazole N atoms and two water O atoms in equatorial positions and the bridging water O atom in the axial position [Cu(1)–O(5) = 2.474(4) Å]. The second Cu^{II} has a similar environment, but it is octahedrally coordinated; the second axial coordination position is achieved by one sulfate O atom [Cu(2)–O(5) = 2.382(5), Cu(2)–O(11) = 2.425(4) Å]. The observed Cu–N distances, ranging from 1.986(5) to 2.005(4) Å, are common for dinuclear *N*1,*N*2-

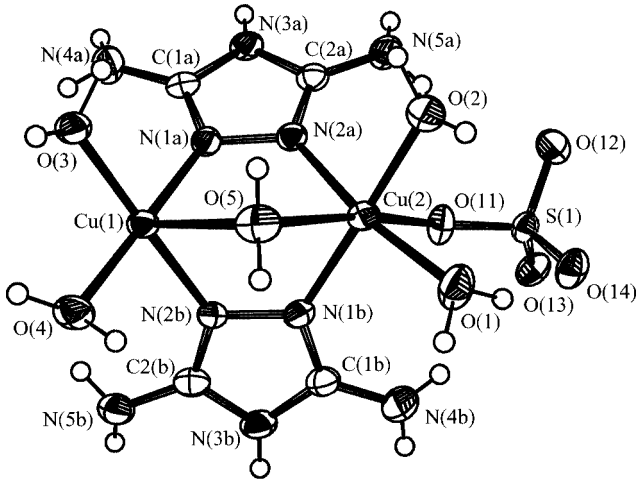

a

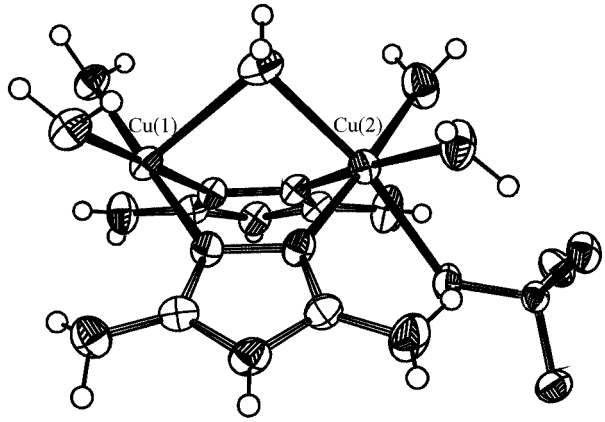

b

Figure 2. ORTEP drawing of **1** showing the atomic labeling system (a) and the noncoplanarity of the $\{Cu(N–N)_2Cu\}$ framework (b).

triazole-bridged Cu^{II} compounds[1,18,19] and comparable to the Cu–O water distances, which range from 1.968(5) to 2.000(4) Å. Cu(1) and Cu(2) are displaced from their corresponding equatorial planes by 0.0104(7) Å and 0.0416(9) Å, respectively. The two equatorial planes are almost perpendicular; the dihedral angle between them measures 80.3(2)°.

The two Cu–O(5) distances differ slightly. The angle Cu(1)–O(5)–Cu(2) is 92.0(2)°. The combination of both bridges gives rise to a Cu···Cu′ distance of 3.4945(8)°. This distance is significantly shorter than that found in double-triazole-bridged Cu^{II} compounds without a third bridge. For example, the Cu···Cu′ distances compiled by Slangen et al.[18] and Ferrer et al.[19] for dimeric compounds oscillate between 4.085(1) and 3.854(6) Å, which indicates that the μ-OH_2 causes the bridging system to fold. It must be taken into account, however, that since the referred compounds all contain *N*,*N*-bridging ligands with N/O-chelating substituents that form five/six-membered chelate rings, the situation is not strictly comparable with that of our structure. In the triazole bridge, the Cu–N–N angles of **1**, which range from 119.9(3) to 123.3(3)°, also differ clearly from those of the aforementioned dimeric Cu^{II} structures, all of which have at least one Cu–N–N angle larger than 128°; besides, those with five-membered chelating rings all have at least two Cu–N–N angles close to 135°.[18,19]

On the other hand, as will be discussed in the next section, the Cu···Cu′ distance of **1** is shorter than the equivalent distance in the analogous linear trinuclear structure of **2** [3.5602(4) Å], which also has an additional small bridge, but a different donor atom size (O_{H_2O} in **1**; Cl^- in **2**).

Another difference between **1** and the dinuclear Cu^{II} complexes mentioned in the literature is that in the latter the {Cu–$(N–N)_2$–Cu} framework is nearly planar,[17] whereas in **1** this group of atoms deviates significantly from planarity (the N atoms deviate from the least-squares plane by 0.8–0.9 Å). In fact, in the double-triazole bridging system of **1**, the dihedral angle between the planes defined by [Cu(1),N(1a),N(2a),Cu(2)] and [Cu(1),N(2b),N(1b),Cu(2)] is 64.3(1)° (Figure 2b).

Complex **1** is, to the best of our knowledge, the second example of a binuclear compound with two bridging triazoles and one bridging oxygen atom. The first example reported, the Cd compound $[Cd_2(deatrz)_2(H_2O)Br_4]$ (deatrz = 3,5-diethyl-4-amino-1,2,4-triazole), forms a 1D chain through hydrogen-bonding contacts.[20] This complex has a Cd···Cd′ distance of 3.819 Å.[21]

Finally, complex **1** presents strong intermolecular hydrogen bonds between the bridging water molecule and the sulfate anions: O(5)–H(w5a)···O(23) (from the non-coordinated sulfate) [2.874(9) Å, 148(5)°] and O(5)–H(w5b)···$O(14^{\#})$ [from the coordinated sulfate of a different asymmetric unit; $O(14^{\#})$ is generated by the symmetry operation: $x - 1/2, -y + 1/2 + 1, + z - 1/2$] [2.723(4) Å, 161(5)°]. Such contacts should play an important role in the stabilization of the structure.

Crystal Structure of $[Cu_3(Hdatrz)_4(\mu\text{-}Cl)_2(H_2O)_4(SO_4)_2]\cdot 11.4H_2O$ (2)

The structure of complex **2** consists of discrete trinuclear entities and randomly placed water of crystallization. The fractional number of water molecules arises from the fact that 2 out of the 7 crystallographically different crystallization water molecules found in the structure do not have a 100% occupancy factor; actually, that of O(5) is 40%, while that of O(9) is only 30%. An ORTEP projection of the structure and the atom-labeling scheme are given in Figure 3. Selected bond lengths and angles are listed in Table 2.

In the linear trinuclear units the metal ions are bridged by two neutral guanazole ligands and one chloride anion. The central copper atom, located at the inversion center, exhibits a tetragonally distorted coordination afforded by four nitrogen atoms from the bridging *N*1,*N*2-triazole ligands and the two bridging chloride anions. Because the copper is situated at the inversion center, the nitrogen atoms are in a nearly regular square, with Cu(2)–N distances of 2.024(3) and 2.003(3) Å. Again, these distances are within

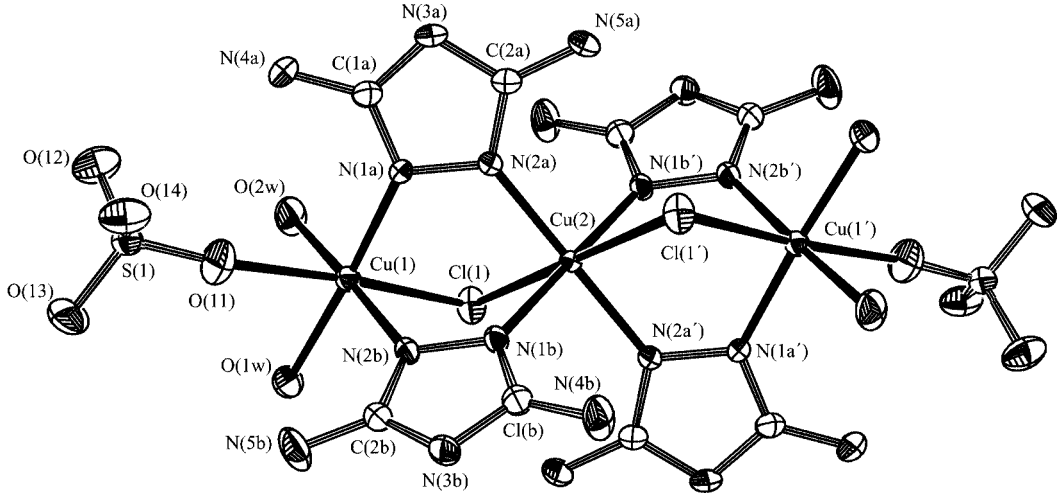

Figure 3. ORTEP drawing of **2** showing the atomic labeling system. H atoms have been omitted for clarity.

Table 2. Selected bond lengths [Å] and bond angles [°] for **2**.[a]

Cu(1)···Cu(2)	3.5602(4)	Cu(1)–N(2b)	1.987(3)
Cu(1)···Cu(1′)	7.120(8)	Cu(1)–N(1a)	1.955(3)
		Cu(1)–O(1w)	2.003(3)
Cu(2)–N(1b)	2.024(3)	Cu(1)–O(2w)	1.977(3)
Cu(2)–N(2a)	2.003(3)	Cu(1)–O(11)	2.511(3)
Cu(2)–Cl(1)	2.785(2)	Cu(1)–Cl(1)	2.624(2)
Cl(1)–Cu(2)–N(1b)	87.91(9)	Cl(1)–Cu(1)–N(2b)	89.25(9)
Cl(1)–Cu(2)–N(2a)	88.03(9)	Cl(1)–Cu(1)–N(1a)	92.22(9)
Cl(1)–Cu(2)–Cl(1′)	180.00(0)	Cl(1)–Cu(1)–O(11)	176.19(8)
Cl(1)–Cu(2)–N(1b′)	92.09(9)	Cl(1)–Cu(1)–O(1w)	92.30(9)
Cl(1)–Cu(2)–N(2a′)	91.97(9)	Cl(1)–Cu(1)–O(2w)	90.26(10)
Cu(1)–Cl(1)–Cu(2)	82.28(3)	N(2b)–Cu(1)–O(1w)	89.1(2)
Cu(1)–N(1a)–N(2a)	122.0(3)	N(1a)–Cu(1)–O(2w)	91.0(2)
Cu(1)–N(2b)–N(1b)	122.3(2)	N(2b)–Cu(1)–N(1a)	91.7(2)
Cu(2)–N(2a)–N(1a)	123.1(2)	O(1w)–Cu(1)–O(2w)	88.2(2)
Cu(2)–N(1b)–N(2b)	122.0(2)	N(1a)–Cu(1)–O(1w)	175.4(2)
N(1b)–Cu(2)–N(2a)	89.4(2)	N(2b)–Cu(1)–O(2w)	177.2(2)
N(1b)–Cu(2)–Cl(1)	87.91(9)	N(2b)–Cu(1)–O(11)	90.00(2)
N(2a)–Cu(2)–Cl(1)	88.03(9)	N(1a)–Cu(1)–O(11)	91.55(2)
N(2a)–Cu(2)–N(1b′)	90.6(2)	O(1w)–Cu(1)–O(11)	83.96(2)
		O(2w)–Cu(1)–O(11)	90.30(2)

[a] Primed atoms are generated by $-x, -y, -z$.

the normal range for *N*1,*N*2-bridging 1,2,4-triazole ligands.[1,18,19,22] The two chloride anions act as axial ligands at semi-coordinating distances [Cu(2)–Cl(1) = 2.785(2) Å]; the distance from the bridging chloride to the terminal metal ion is comparable [Cu(1)–Cl(1) = 2.624(2) Å]. Thus, the chlorido bridge, with a Cu(1)–Cl(1)–Cu(2) angle of 82.28(3)°, is rather symmetrical.

The chlorido bridging system of **2** is different from that found in the analogous compound reported by van Koningsbruggen et al., $[Cu_3(H_2ahmt)_6Cl_4]Cl_2$ [H_2ahmt = 4-amino-3,5-bis(hydroxymethyl)-1,2,4-triazole] (compound **6**, Table 3), in which not only are the μ-Cl^- located at equatorial instead of axial positions in the environment of the central Cu^{II}, but also the bridging distances are very asymmetric [Cu(1)–Cl(1) = 2.296(1), Cu(2)–Cl(1) = 2.688(1) Å].[22] This situation is probably related to the steric hindrance produced by bulkier substituents on the ring of the H_2ahmt ligand. In contrast, **2** is more comparable with the compound described by Keij and co-workers, $[Cu_3(tmtz)_8F_2](BF_4)_4{\cdot}2H_2O$ [tmtz = 3,4,5-trimethyl-1,2,4-triazole] (**7**), although the latter has one F^- instead of one Cl^- bridge [Cu(1)–F(1) = 2.20(1), Cu(2)–F(1) = 1.91(1) Å].[23]

The terminal copper ions of **2** are hexacoordinated by two nitrogen atoms from bridging triazole ligands and two oxygen atoms from two water molecules, all in equatorial positions, and by the bridging chloride anion and an oxygen atom from a sulfate anion in apical positions [Cu(1)–O(1) = 2.511(3) Å]. The Cu(1)(terminal)–N distances [1.995(3), 1.987(3) Å] are slightly shorter that the Cu(2)(central)–N distances [2.003(3), 2.024(3) Å], but it can be considered that the H_2datrz ligands also bridge the copper(II) ions in an almost symmetrical way, as evidenced by the close values of the Cu–N–N angles, which range from 122.0(3) to 123.1(2)°, and those of the N–Cu–N angles, with values of 89.4(2) and 91.7(2)°. The Cu–N–N–Cu torsion angles [–4.2(4) and –9.4(4) Å], indicate that the triazole ligands tend to twist out of the equatorial plane formed by the two Cu^{II} ions involved.

The equatorial coordination planes around Cu(1) and Cu(2) form a dihedral angle of 79.0(1)°. Thus, they are almost perpendicular, as was also observed in the dimeric structure of **1**. The dihedral angle between the least-squares planes through the triazole rings linking Cu(1) and Cu(2) measures 55.7(2) Å (Figure 3).

The Cu(1)–Cu(2) distance is 3.5602(4) Å, which is similar to that found in related linear trinuclear double-μ-*N*1,*N*2-triazole-bridged Cu^{II} complexes with an additional small bridging anion such as Cl^- [3.5426(1), 3.620(3), and 3.5682(5) Å, for complexes **3**, **4**, and **6**, respectively][22,24] or N_3^- [3.5034(6) Å for **5**],[25] but longer than that of the analogous complex with an F^- bridge [3.362(3) Å for **7**].[23] This is probably due to the small size of the F^- ion (Table 3). It should be noted that the Cu···Cu′ separation in **2** is shorter than that in triple-μ-*N*1,*N*2-triazole-bridged copper(II) compounds, such as $[Cu_3(metrz)_6(H_2O)_4](CF_3SO_3)_6{\cdot}4H_2O$ (metrz = 3-methyl-4-ethyl-1,2,4-triazole) [3.719(7) Å][26] or $[Cu(hyetrz)_3](ClO_4)_2{\cdot}3H_2O$ [hyetrz = 4-(2-hydroxyethyl)-1,2,4-triazole] [3.853(2) and 3.829(2) Å].[27] This indicates that, when the third triazole is replaced by monatomic bridges, the Cu···Cu′ distance tends to shorten, as previously reported[25,27] and, indeed, as expected due to the larger size of the third bridge.

Table 3. Magnetic and structural parameters in linear trinuclear double-(μ-*N*1,*N*2-triazole)-bridged Cu^{II} complexes with a small additional bridge.

Complex[a]	Cu(2)···Cu(1) [Å]	Cu(2)–A[b]–Cu(1) [°]	Cu(1)–N(1a) Cu(1′)–N(1a′) [Å]	Cu(1)–N(2b) Cu(1′)–N(2b′) [Å]	Cu(2)–N(1b) Cu(2)–N(1b′) [Å]	Cu(2)–N(2a) Cu(2)–N(2a′) [Å]	*J* [cm^{-1}]	Ref.
$[Cu_3(Hdatrz)_4Cl_2(H_2O)_4(SO_4)_2]{\cdot}11.4H_2O$ (**2**)	3.5602(4)	82.28(3)	1.995(3)	1.987(3)	2.024(3)	2.00(3)	–89.9	this work
$[Cu_3(attn)_2Cl_2(H_2O)_2]Cl_4{\cdot}4H_2O$ (**3**)	3.5426(1)	84.013(9)	2.023(1)	2.003(1)	2.040(1)	1.985(1)	–75.1	[24]
$[Cu_3(attn)_2Cl_2(ZnCl_4)_2]$ (**4**)	3.620(3)	80.6(1)	1.98(1)	1.99(1)	2.04(1)	1.98(1)	–70.9	[24]
$[Cu(atrz)_2(N_3)](NO_3)$ (**5**)	3.5034(6)	104.05(12)	2.402(3)	2.008(3)	2.011(3)	2.029(3)	–35.4	[25]
$[Cu_3(H_2ahmt)_6Cl_4]Cl_2$ (**6**)	3.5682(5)	91.09(4)	1.966(3)	2.079(4)	2.023(3)	2.554(3)	–33.8	[22]
$[Cu_3(tmtz)_8F_2](BF_4)_4{\cdot}2H_2O$ (**7**)	3.362(3)	–	2.24(2)	2.01(1)	2.05(1)	2.04(1)	–	[23]

[a] Hdatrz = 3,5-diamino-1,2,4-triazole; attn = 1,9-bis(3-aminotriazol-5-yl)3,7-dithianonane; atrz = 4-amino-1,2,4-triazole; H_2ahmt = 4-amino-3,5-bis(hydroxymethyl)-1,2,4-triazole; tmtz = 3,4,5-trimethyl-1,2,4-triazole. [b] A = Cl^-, $N(N_3^-)$, F^-.

We have carried out a review of the literature in order to compare more systematically some structural parameters of **2** with those of analogous compounds. Several linear trinuclear coordination compounds of this type, i.e. containing *two* 1,2,4-triazole ligands bridging through *N*1,*N*2 atoms and either a halogen anion or a second small bridging anion, have been previously reported: (a) three Co^{II} compounds with F^-[28,29] or *N*-bridging NCS^- ligands,[30] (b) three Ni^{II}–*N*(NCS^-) compounds,[30–32] (c) one Mn(II,III,II) complex with hydroxido bridges,[33] (d) two Cd^{II} compounds containing Cl^-[20] or *N*,*N*-isothiocyanato bridges,[20] and (e) a few Cu^{II} compounds (Table 3). The first structurally characterized (triazole)copper(II) compound to include μ-chloride ions was [{Cu(Htrz)Cl_2}$_\infty$], but it consists of an infinite chain with two Cl^- and a *single* triazole ligand per pair of copper atoms instead of one Cl^- and two triazole ligands.[34] To the best of our knowledge, only five Cu^{II} compounds strictly comparable to **2** as regards bridging systems have been published to date (all have been mentioned above): one containing μ-fluoride anions (**7**),[23] three with chlorido bridges (**3**, **4**, and **6**; of which **3** and **4** have an unusual chelating tetradentate triazole ligand), and one in which the small bridging anion is the azido N_3^- group (**5**).[25] Table 3 lists several structural parameters, including coordination distances, which will be considered in the magnetism section.

Magnetic Properties

Magnetic Properties of 1

Figure 4 displays the magnetic behavior of **1** in the form of a $\chi_M T$ and χ_M vs. *T* plot, where χ_M is the magnetic susceptibility per two Cu^{II} ions. Upon cooling, the $\chi_M T$ values decrease continuously from room temperature (0.73 $cm^3 \cdot mol^{-1} \cdot K$) until they vanish at 20 K. The χ_M curve shows a maximum at 90 K. This behavior is characteristic of an antiferromagnetic interaction between Cu^{II} ions with a singlet spin ground state.

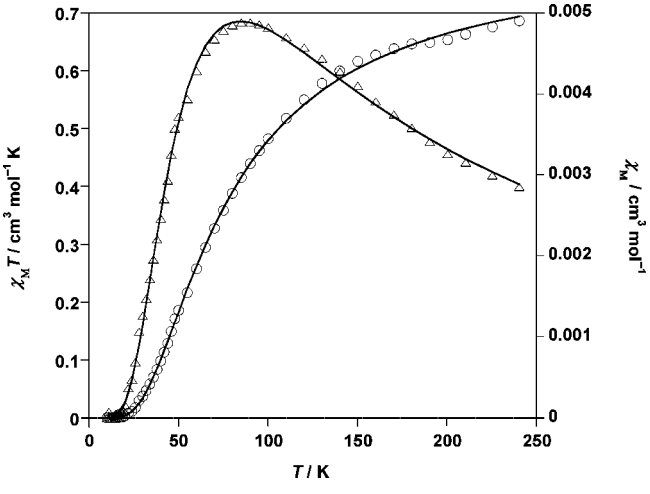

Figure 4. Thermal dependence of $\chi_M T$ (○) and χ_M (Δ) for **1** (solid lines represent theoretical curves, see text).

The magnetic data have been interpreted in accordance with the actual dinuclear nature of the complex by using the spin Hamiltonian $\mathbf{H} = -J\mathbf{S}_1\mathbf{S}_2$, from which the following susceptibility equation can be derived [Equation (1)]:

$$\chi_M = \frac{2N\beta^2 g^2}{kT} \frac{1}{3 + \exp(-\frac{J}{kT})} \quad (1)$$

Assuming that the *g* factors for both Cu^{II} atoms are identical, the fit of the magnetic data with this expression results in $g = 2.10(1)$ and $J = -94.3(2)$ cm^{-1}.

From the molecular structure, it could be concluded that the magnetic exchange occurs via the $d_{x^2-y^2}$ orbitals on the Cu^{II} ions that overlap with the σ orbitals of the nitrogen atoms of the triazole bridges, which are placed at equatorial positions. Exchange interaction through the pathway provided by the large axial bonding (through the μ-OH_2) can be expected to have little relevance (see Figure 2b) because of the low unpaired electron density along de d_{z^2} orbital in the octahedral coordination around the copper atoms. In principle, then, at least from a magnetic point of view, compound **1** could be compared to related bis(μ-triazole)-bridged Cu^{II} complexes.

Although the literature contains many examples of copper(II) complexes with bridging triazole or triazolate functionalities, only 15 acyclic complexes with metal centers bridged by two triazole-triazolate units have been structurally characterized to date,[18,19,36–42] and for only 10 of these has a magnetic study been performed; Table 4 offers a compilation of these studies.[18,19,35–39,41] As a first attempt at establishing magneto-structural correlations, Haasnoot and co-workers,[18] working with a set of compounds, concluded that Cu–N_{trz}–N_{trz} angles of 134–135° in symmetrically doubly bridged systems lead to the largest possible coupling, with $|J| \approx 240$ cm^{-1}. Table 4, however, shows that, taken separately, neither the symmetry nor the Cu–N_{trz}–N_{trz} angles allow for a prediction of the magnitude of the exchange coupling. The last two compounds in Table 4, both of which exhibit fairly symmetrical {Cu–N–N}$_2$ frameworks, present the lowest $|J|$ values. Moreover, in spite of its smaller Cu–N_{trz}–N_{trz} angles, compound **1** displays an absolute value for *J* that is larger than that for [Cu(daat)-(NO_3)(H_2O)]$_2$. In this context, and with the aim of determining the factors that dominate the magnetic interaction, we carried out several DFT calculations. Trials with models including fixed Cu–N distances and variable bridging angles turned out to be unsuccessful in that they could not reproduce the trend of the experimental *J* values. In fact, the only conclusion was that the bridging angles are related with, but do not determine, the *J* value, as we had already deduced from Table 4. On the other hand, it should be noticed that, as mentioned above, in all the previously reported complexes, the [Cu_2L_2] unit is planar; compound **1** is the only described instance of a folded dicopper(II) complex with acyclic triazole ligands.[43] In a series of closely related dicobalt(II) complexes, a decrease in magnetic exchange interactions was observed for folded dico-

Table 4. Magnetic and structural parameters in the $\{Cu–N–N\}_2$ ring for dinuclear double-(μ-*N*1,*N*2-triazole)-bridged copper(II) compounds.[18,19].

Compound[a]	N(1a)–Cu(1)–N(2b) [°][b]	Cu(2)–N(2a)–N(1a) [°][b]	Cu(1)–N(1a)–N(2a) [°][b]	Cu···Cu′ [Å]	$-J$[c] [cm^{-1}]	Ref.
$[Cu(bpt)(CF_3SO_3)(H_2O)]_2$	90.2(1)	134.7(2)	135.0(2)	4.085(1)	236	[35]
$[Cu(aamt)Br(H_2O)]_2Br_2·2H_2O·CH_3OH$	92.1(1)	134.2(2)	133.7(2)	4.0694(7)	220	[36]
$Cu_2(ibdpt)_2(ClO_4)_4(MeCN)$	92.7(2)	133.8(3)	133.5(3)	4.070(1)	210[d]	[41]
$[Cu(aamt)(H_2O)_2]_2(SO_4)_2·4H_2O$	91.9(4)	135.1(8)	132.9(8)	4.088(3)	194	[37]
$[Cu^{II}(maamt)(Cu^{I}Cl_3)]_2$	–	133.0(4)	133.9(3)	4.048(1)	156	[39]
$[Cu_2(pt)_2(4,4'\text{-bpy})(NO_3)_2(H_2O)_2]·4H_2O$	95.5(1)	139.4(2)	125.2(2)	4.0198(7)	102	[38]
$[Cu_2(pt)_2(SO_4)(H_2O)_3]·3H_2O$	94.7(2)	139.8(3)	124.9(3)	4.0265(8)	98	[18]
$[Cu_2(pt)_2(Hpz)_2(NO_3)_2(H_2O)_2]$	96.5(2)	139.6(3)	123.9(3)	3.974(1)	98	[38]
$[Cu_2(pt)_2(Meim)_2(NO_3)_2(H_2O)_2]·4H_2O$	95.4(1)	138.7(2)	125.8(2)	4.022(1)	96	[38]
$[Cu_2(Hdatrz)_2(\mu\text{-}OH_2)(H_2O)_4(SO_4)](SO_4)·3.5H_2O$ (**1**)	92.4(2)	122.2(3)	120.8(3)	3.495(8)	94	this work
$[Cu(daat)(NO_3)(H_2O)]_2$	102.8(5)	128.0(8)	129.2(8)	3.832(1)	72	[19]

[a] bpt = 3,5-bis(pyridin-2-yl)-1,2,4-triazolate; aamt = 4-amino-3,5-bis(aminomethyl)-1,2,4-triazole; ibdpt = 4-isobutyl-3,5-bis(2-pyridyl)-4*H*-1,2,4-triazole; maamt = 4-amino-3,5-bis[(*N*-methylamino)methyl]-1,2,4-triazole; pt = 3-pyridin-2-yl-1,2,4-triazolate; 4,4′-bpy = bipyridine; Hpz = pyrazole; Meim = *N*-methylimidazole; daat = 3,5-bis(acetylamino)-1,2,4-triazolate. [b] Averaged values. [c] Values from literature adapted according to definition used in this work [see Equation (1)]. [d] Measurements performed on partially desolvated sample (and in the presence of some monomeric impurities).

balt(II) complexes as compared to their planar analogues.[43,44] This behavior is reasonable since the distortion leads to less overlap between the magnetic orbitals of the metal centers and the σ orbital of the ligand. In contrast, compound **1** exhibits larger coupling than the planar $[Cu(daat)(NO_3)(H_2O)]_2$ compound, thereby excluding coplanarity as a main factor in the magnitude of the interaction. In summary, several parameters seem to influence the magnetic exchange in the double-triazole-bridged dinuclear compounds; more examples are needed to derive a clear magneto-structural relationship.

Magnetic Properties of 2

The magnetic behavior of **2** is depicted in Figure 5 in the form of a $\chi_M T$ vs. T plot, where χ_M is the magnetic susceptibility per three Cu^{II} ions. At room temperature, the $\chi_M T$ value is 1.00 $cm^3·mol^{-1}·K$. Upon cooling, the $\chi_M T$ values decrease, reaching a plateau with a value of 0.43 $cm^3·mol^{-1}·K$ at approximately 25 K. This behavior is characteristic for compounds with an overall antiferromagnetic interaction between the Cu^{II} ions, which induces a spin doublet ground state.

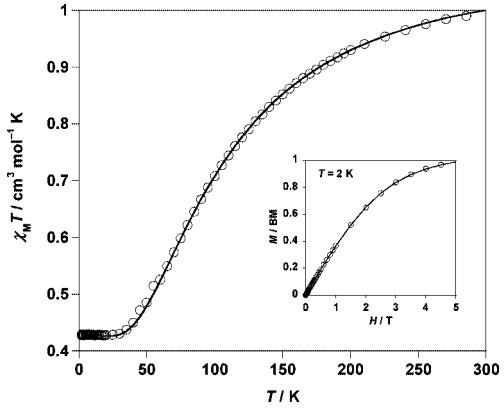

Figure 5. Thermal dependence of $\chi_M T$ for **2** (the solid line represents the theoretical curve, see text). The inset displays the magnetization curve at 2 K for **2** (the solid line is drawn to guide the eye).

In order to obtain the relevant magnetic parameters, the experimental data have been fitted by using Equation (2), derived from the spin Hamiltonian $\mathbf{H} = -J(\mathbf{S}_1\mathbf{S}_2 + \mathbf{S}_2\mathbf{S}_3)$, where $\mathbf{S}_1$ and $\mathbf{S}_3$ correspond to the peripheral Cu^{II} ions ($g_1 = g_3 = g_p$) and $\mathbf{S}_2$ to the central one ($g_2 = g_c$).

$$\chi_M = \frac{N\beta^2}{4kT}\frac{g_{1/2,1}^2 + g_{1/2,0}^2\exp(\frac{J}{kT}) + 10g_{3/2,1}^2\exp(\frac{3J}{2kT})}{1+\exp(\frac{J}{kT})+2\exp(\frac{3J}{2kT})} \quad (2)$$

where:

$$g_{1/2,1} = \frac{4g_p - g_c}{3}$$
$$g_{3/2,1} = \frac{2g_p + g_c}{3} \quad (3)$$
$$g_{1/2,0} = g_c$$

The exchange constant between the terminal copper ions is assumed to be negligible. This assumption is justified from the study of the triple triazole-bridged Fe^{II}–Fe^{II}–Fe^{II}[45] and Co^{II}–Co^{III}–Co^{II}[13] trinuclear clusters, in which the central metal ion is diamagnetic, and no magnetic interactions are detected between the paramagnetic terminal ions. Moreover, these interactions only affect the relative position of the excited spin doublet with respect to the ground spin doublet and the excited spin quartet. The effect of these interactions on magnetic properties, if any, is insignificant.[46,47]

The best-fit parameters obtained were: $J = -89.9(3)$ cm^{-1}, $g_{central} = 2.12(1)$, and $g_{peripheral} = 2.07(1)$. The J value of **2** is thus very similar to that observed for the dinuclear compound **1**, as could be expected from the identical nature of the main bridge and the similar distortion of the cores (the dihedral angles between the equatorial Cu^{II} planes are 80° in **1** and 79° in **2**).

Selected magneto-structural data for the known linear trinuclear Cu^{II} compounds with double μ-triazole bridges and an additional small bridge are listed in Table 3. Two groups of compounds can be established from the magnitude of the exchange: (a) those with J values around –75 cm^{-1} (compounds **2**–**4**), and (b) those with J values close to –34 cm^{-1} (compounds **5** and **6**). This trend in the J values can be understood on the basis of simple orbital symmetry considerations (see Figure 6) and also by taking into account that the magnitude of the antiferromagnetic coupling, J_{AF}, is proportional to the overlap integral between the magnetic orbitals.[48]

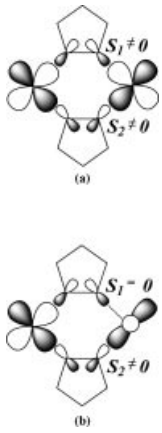

Figure 6. Orbital models for the triazole bridging system.

For compounds **2**–**4** (Figure 6a), in which both triazole bridges are located at equatorial positions as deduced from the coordination distances (see Table 3), the unpaired electron on each Cu^{II} ion is in a $d_{x^2-y^2}$ type magnetic orbital, where the x and y axes are roughly described by the copper–$N_{triazole}$ bonds. Both magnetic orbitals exhibit good sigma overlap on each side of the bridge. As for compounds **5** and **6** (Figure 6b), only one triazole bridge is at an equatorial position (see coordination distances in Table 3). As a consequence, one of the magnetic orbitals (that corresponding to the axial site) is reversed and thus perpendicular to the triazole ring, whereas the other magnetic orbital remains coplanar. Because of the relative orientation of these magnetic orbitals, the interaction only occurs through one side of the bridge. The experimental J values for both groups of compounds, that is, around –75 cm^{-1} for **2**–**4** and around –34 cm^{-1} for **5** and **6**, are in agreement with this simple orbital model.

Spectroscopic Properties

IR Spectra

The IR spectrum of guanazole has already been studied in detail by Desseyn et al.[9] and Kumar et al.[49] The assignment of the main peaks of the ligand and complexes **1** and **2** is indicated in the experimental section. Especially noteworthy is the fact that the IR spectra of both compounds are almost indistinguishable; this is related to the similarity in the coordination of the ligand and to the presence of similar IR-active groups such as uncoordinated and/or monocoordinated sulfate and coordinated and uncoordinated water molecules in both **1** and **2**. A minor difference is observed in the first band of the spectrum (at around 3400 cm^{-1}), which appears at a higher frequency in **1** than in **2**. This could be attributed to the vibrations of the μ-OH_2 bridge. Characteristic absorbances in agreement with both coordinated (C_{3v} symmetry) and uncoordinated sulfate can be appreciated in the spectra of both complexes.[50]

Electronic Spectra

The UV/Vis spectra of both compounds, recorded by using solid samples (diffuse-reflectance technique), show asymmetric bands centered at around 700 nm (**1**) and 710 nm (**2**). This feature is in agreement with the presence of two different chromophores in each complex and with the distorted tetragonal (square-pyramidal or octahedral) geometry of the copper(II) ions present in the two structures.[51] Furthermore, a clearly distinguishable maximum is observed at ca. 400 nm (**1**) and ca. 415 nm (**2**), which could be attributed either to a charge-transfer band or, in the case of **1**, to the high-energy absorption for copper(II) dimers frequently present in this region of the spectra.[19,35,52,53]

EPR Spectra

Powder EPR spectra of the complexes have been recorded at room temperature at the X-band frequencies (0–5000 G), and from room temperature to 4 K at the Q-band frequencies (0–15000 G). To exclude the presence of impurities, different measurements were performed with samples obtained by powdering single crystals from different preparations. Figure 7 (for **1**) and Figure 8 (for **2**) exhibit selected Q-band spectra.

The room-temperature X-band EPR spectrum of **1** exhibits a very weak half-field ($\Delta M_s = \pm 2$) signal, centered at 1550 G, typical of a spin-coupled binuclear copper(II) system with significant population at the triplet state. An isotropic $\Delta M_s = \pm 1$ transition is also observed at $g = 2.16$. As for the Q-band frequencies, the room-temperature spectrum of **1** can be described either as inverted axial or as slightly rhombic (Figure 7a). No signal corresponding to the forbidden transition (around 4000 G) could be detected. At lower temperatures, the spectrum becomes progressively more resolved. At 30 K (Figure 7b), the spectrum shows an anisotropic signal at 10910 G and a signal at 11960 G, which can be assigned to one of the perpendicular and parallel transitions, respectively, of the excited triplet state ($S = 1$).[51] Finally, as expected, the spectrum vanishes below 30 K because of the antiferromagnetic interaction in the dimer, which leads to a diamagnetic $S = 0$ state.

The exchange interaction parameter J can be determined from the temperature variation of the EPR absorption lines. The relative intensity of the absorption is expressed by Equation (3):[54]

$$R \propto (1/T)\,[(e^{-J/kT})/(1 + 3\,e^{-J/kT})] \quad (3)$$

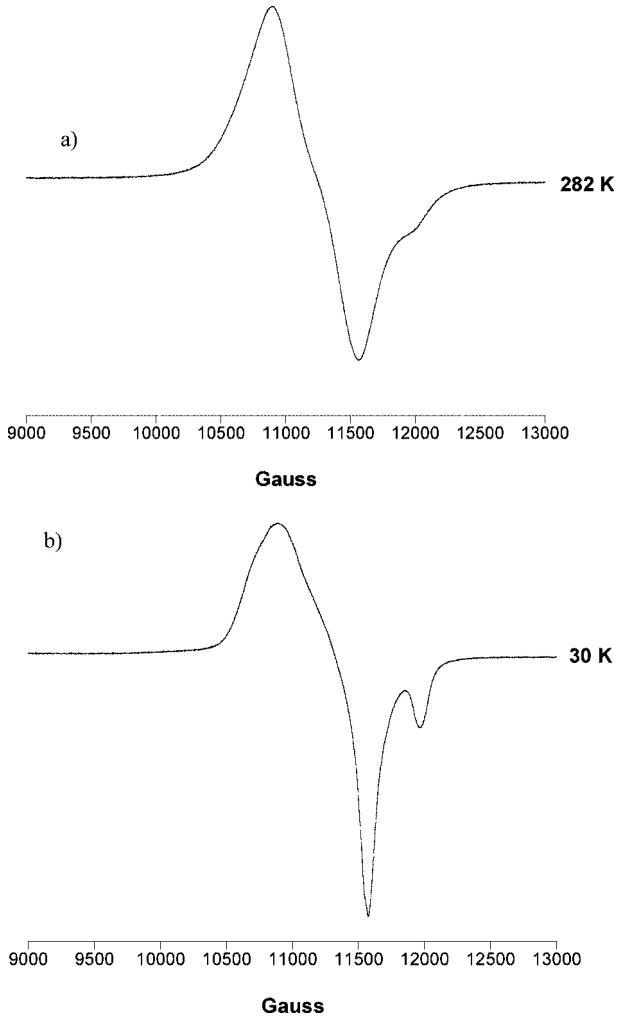

Figure 7. EPR for **1** at (a) 282 K and (b) 30 K.

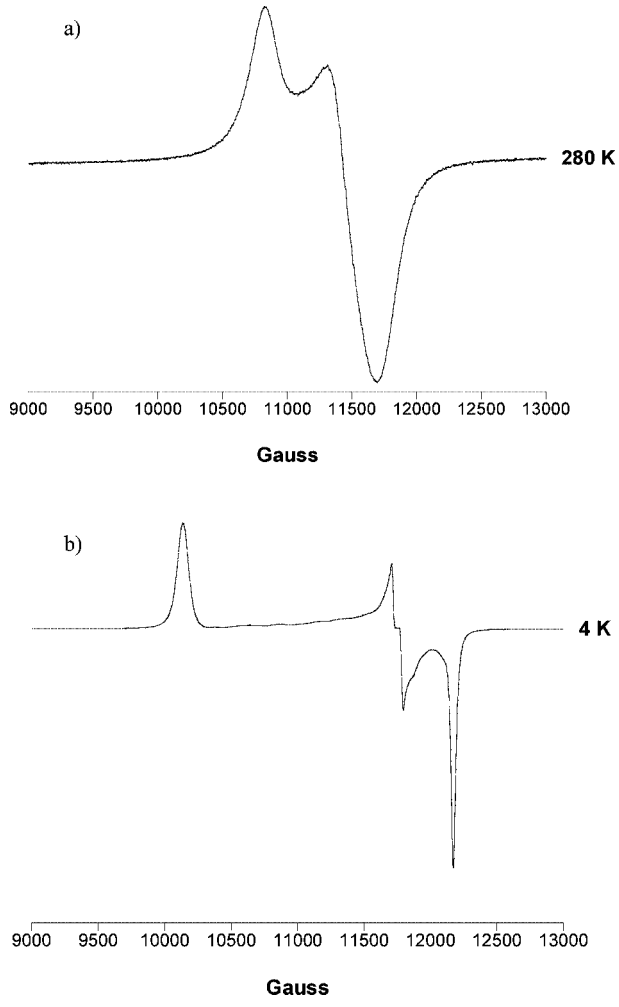

Figure 8. EPR for **2** at (a) 280 K and (b) 4 K.

This approach was applied to compound **1**. A value of $-J = 89\ cm^{-1}$ was obtained, which is very close to the value calculated from the magnetic measurements [$J = -94.3(2)\ cm^{-1}$].

For **2**, the X-band EPR spectrum recorded at room temperature is isotropic, with a signal centered at $g = 2.13$. The room temperature Q-band spectrum is axial (Figure 8a). At lower temperatures, the signals become better defined and the spectra are rhombic. Figure 8b displays the spectrum at 4 K; it is clearly rhombic, with signals at $g_3 = 2.39$, $g_2 = 2.07$, and $g_1 = 2.00$, which is in agreement with both the stereochemistry of the copper(II) ions[51] and the spin doublet ground state.[55]

Concluding Remarks

Control of appropriate conditions for synthesis has permitted the isolation of two Cu^{II} compounds of guanazole, **1** and **2**, with different nuclearity. To the best of our knowledge, these compounds represent the first structurally characterized Cu^{II} compounds of this ligand. In both cases, the guanazole acts in its neutral form through its *N*1,*N*2-bidentate bridging mode. While compound **1** is dimeric, **2** is a linear trinuclear complex. The two copper atoms in **1**, and the two nearest copper atoms in **2**, are linked by double triazole bridges and by a third, small H_2O (in **1**) or Cl^- (in **2**) bridge. Compound **1** is the second reported case of a compound that uses triazole ligands together with μ-OH_2 as bridges.[21]

For both compounds, a significant antiferromagnetic interaction of similar magnitude [$J = -94.3(2)\ cm^{-1}$ (**1**), $J = -89.9(3)\ cm^{-1}$ (**2**)] has been observed. This is in agreement with the similarity of the bridging triazole systems, which comprise the main exchange pathways. Compound **1** has presented us with the opportunity of testing the influence of a nonplanar $\{Cu(N–N)_2Cu\}$ framework on the magnitude of the AF exchange. For its part, compound **2** exhibits one of the largest magnetic exchange constants found in linear trinuclear double/triple-triazole bridged Cu^{II} complexes to date; this has likewise been rationalized for the first time in terms of simple orbital symmetry models.

Experimental Section

Instrumentation: Elemental analyses were performed with a CE EA 1110 CHNS instrument. Infrared spectra were recorded with a Mattson Satellite FT-IR spectrophotometer from 4000 to 400 cm^{-1} by using KBr disks. Ligand field spectra were obtained from 800 to 200 nm with a Shimadzu 2101-PC UV/Vis instrument, by using the diffuse-reflectance technique, with Nujol mulls. EPR spectra of powdered samples were collected on a Bruker ELEXSYS spectrometer at variable temperature operating at Q-band frequencies, and at room temperature operating at X-band frequencies. Magnetic susceptibility measurements of polycrystalline samples were measured over the temperature range 2–300 K with a Quantum Design SQUID magnetometer by using an applied magnetic field of 1000 G. Diamagnetic corrections of the constituent atoms were estimated from Pascal's constants. Experimental susceptibilities were also corrected for the temperature-independent paramagnetism [-60×10^{-6} $cm^3 \cdot mol^{-1}$ per copper(II)] and for the magnetization of the sample holder.

Chemicals: The guanazole ligand (Hdatrz) was obtained from Janssen Chimica. The 3,5-diacetylamino-1,2,4-triazole ligand (Hdaatrz) was prepared as indicated by van den Bos[56] and recrystallized from boiling water. Copper salts and solvents of high purity were commercially available and used as such.

Synthesis of $[Cu_2(Hdatrz)_2(\mu\text{-}OH_2)(H_2O)_4(SO_4)](SO_4)\cdot 3.5H_2O$ (1): (a) Copper(II) sulfate (6 mmol, 1.52 g) and Hdaatrz (1 mmol, 0.14 g) were mixed in water (40 mL) with continuous stirring. The resulting green solution was allowed to stand at room temperature. In about one month, a precipitate appeared which was filtered off, and the resulting solution was kept in the freezer. After about six months, large, green, hexagonal prism-shaped crystals of **1** (ca. 0.23 g, 70%) were observed together with a few smaller, lighter green crystals. Crystals of **1** were manually isolated on filter paper. One of those crystals was selected for X-ray measurements. The X-ray analysis revealed that Hdaatrz, in the presence of a high proportion of aqueous copper(II) [Cu^{II}:Hdaatrz is 6:1], had undergone hydrolysis to form a (guanazole)copper(II) compound. (b) Single crystals of **1** could also be obtained directly from guanazole as follows: Copper(II) sulfate (1 mmol, 0.25 g) was added to a hot aqueous solution of guanazole (1 mmol, 0.10 g, in 30 mL) with continuous stirring (so that the ratio Cu^{II}: guanazole is 1:1). A precipitate was immediately formed, which was separated by filtration. The resulting green solution was allowed to stand at room temperature. After ca. one month, single crystals of **1** (ca. 0.10 g, 30%) appeared together with other brownish green, needle-shaped crystals. Crystals of **1** were manually isolated on filter paper. The synthesis from guanazole (b) gave a lower yield than that from Hdaatrz (a).

Synthesis of $[Cu_3(Hdatrz)_4(\mu\text{-}Cl)_2(H_2O)_4(SO_4)_2]\cdot 11.4H_2O$ (2): Copper(II) sulfate (0.5 mmol, 0.13 g) was mixed with a hot aqueous solution of guanazole (1 mmol, 0.10 g, in 30 mL) with continuous stirring. A precipitate was formed immediately. Then, copper(II) chloride (3 mmol, 0.51 g) was added to the suspension, and the precipitate was redissolved (so that the ratio Cu^{II}:Hdatrz was 3.5:1). The resulting brownish green solution was allowed to stand in the freezer. After less than one week, large, dark green, prism-shaped crystals of **2** (ca. 0.10 g, 70%) were observed and isolated on filter paper. These crystals, however, are unstable at room temperature and turn to powder after ca. one hour after being taken out of the freezer, due to water loss (as indicated by the corresponding elemental analysis). So, all analyses and measurements had to be performed directly after isolation of the crystals.

Analysis: For **1**: $C_4H_{27}Cu_2N_{10}O_{16.5}S_2$ (670.56): calcd. C 7.16, H 4.06, N 20.89, S 9.56; found C 7.37, H 4.20, N 21.02, S 10.01 (on the sample synthesized by method b). Crystals of **1** from synthesis (a) were only analyzed by X-ray diffraction (Table 5). For **2**: $C_4H_{25.4}Cl_1Cu_{1.5}N_{10}O_{11.7}S_1$ (563.76): calcd. C 8.52, H 4.54, N 24.85, S 5.69; found C 8.27, H 4.85, N 24.46, S 5.70.

Spectroscopy

$\tilde{\nu}_{max}$ for Hdatrz: [$\upsilon(N\text{–}H)_{NH,NH_2}$] 3398 (m), 3368 (sh), 3312 (m), 3237 (w); [υ(C=N)/ring stretching vibrations + $\delta(N\text{–}H)_{NH,NH_2}$] 1628 (vs), 1582–1563 (split,s), 1489 (s), 1417 (s); other peaks: 1346 (m), 1152 (w), 1126 (w), 1064 (m), 1015 (w), 808 (m), 727 (w), 647–616 (broad,m), 539 (w) cm^{-1}.

λ_{max} (solid sample, diffuse-reflectance technique) for **1**: ca. 400, ca. 700 nm; $\tilde{\nu}_{max}$ for **1**: [$\upsilon(O\text{–}H)_{H2O}$ + $\upsilon(N\text{–}H)_{NH,NH_2}$] 3426 (m); [$\upsilon$(C=N)/ring stretching vibrations + $\delta(N\text{–}H)_{NH,NH_2}$] 1705 (sh), 1663–1644(split,s); [$\upsilon_3(SO_4)$] 1187 (sh), 1115 (vs); [$\upsilon_4(SO_4)$] 620 (m) cm^{-1}.

λ_{max} (solid sample, diffuse-reflectance technique) for **2**: 415, ca. 710 nm; $\tilde{\nu}_{max}$ for **2**: [$\upsilon(O\text{–}H)_{H2O}$ + $\upsilon(N\text{–}H)_{NH,NH_2}$] 3407–3315(br,m); [$\upsilon$(C=N)/ring stretching vibrations + $\delta(N\text{–}H)_{NH,NH_2}$] 1647 (vs); [$\upsilon_3(SO_4)$] 1195 (w), 1115 (s), 1061 (sh); [$\upsilon_4(SO_4)$] 624 (m) cm^{-1}.

Crystal Structure Determination: Crystallographic data for **1** and **2** are summarized in Table 5. One light green (**1**) and one dark green (**2**) prism-shaped crystal were selected. That of **2** was mounted with Vaseline on a capillary. Throughout the experiment Cu-K_α (**1**) or Mo-K_α (**2**) was used with a graphite crystal monochromator on a Nonius Kappa-CCD [λ = 1.54184 Å (**1**); λ = 0.71073 Å (**2**)] single-crystal diffractometer. Unit cell dimensions were determined from the angular settings of 4343 (**1**) and 3966 (**2**) reflections with θ between 0.883° to 70.076° (**1**) and 0.998° to 27.485° (**2**), and refined with the programs HKL Denzo and Scalepack.[57] Space groups were determined to be monoclinic $C2/c$ (**1**) or triclinic $P\bar{1}$ (**2**), from systematic absences (**1**) or from structure determination (**2**). Crystal-detector distance was fixed at 30 mm, and a total of 1732 (**1**)/183 (**2**) images were collected by using the oscillation method, with scan angle per frame 2° oscillation and 5 s exposure time per image. The data collection strategy was calculated with the program Collect.[58] Structure **1** was solved by using DIRDIF;[59] structure **2** by using SIR97;[60] isotropic least-squares refinements on F^2 were made by using SHELX97;[61] during the final stages of refinements on F^2 the positional parameters and the anisotropic thermal parameters of the non-H atoms were refined. Some hydrogen atoms were located by Fourier difference synthesis and the rest were geometrically placed. H atoms on triazole N atoms were found in a Fourier map for **1** and geometrically placed in **2**. The final difference Fourier map for **1** showed the highest peaks of 2.055 e A^{-3} at 1.41 Å from O(24) and of 1.89 e A^{-3} at 1.25 Å from O(21); the rest of them were lower than 0.67 e A^{-3}, the deepest hole being –1.109 e A^{-3} at 0.62 Å from Cu(1). The same map for **2** showed the highest peak of 1.044 e A^{-3} at 0.7 Å from O(5w) and the deepest hole of –0.723 e A^{-3} at 0.14 Å from H(6a). Figure 1 and Figure 2, made with ORTEP,[62] show the atomic numbering schemes. Atomic scattering factors were taken from ref.[63]. Geometrical calculations were made with PARST.[64] CCDC-293618 (**1**) and CCDC-293619 (**2**) contain the supplementary crystallographic data for this paper. These data can be obtained free of charge from The Cambridge Crystallographic Data Centre via www.ccdc.cam.ac.uk/data_request/cif.

Table 5. Crystallographic data and structure refinement for compounds **1** and **2**.[a]

Compound	**1**	**2**
Empirical formula	$C_4H_{27}Cu_2N_{10}O_{16.5}S_2$	$C_4H_{25.4}Cu_{1.5}N_{10}O_{11.7}S_1Cl_1$
Formula weight	670.56	563.76
Temperature [K]	293(2)	293(2)
Wavelength [Å]	1.54184	0.71073
Crystal system, space group	monoclinic, *C*2/c	triclinic, $P\bar{1}$
a [Å]	19.0944(4)	10.2780(2)
b [Å]	21.3853(4)	10.5110(2)
c [Å]	14.4018(3)	11.4020(2)
α [°]		77.6520(12)
β [°]	129.8510(10)	63.3760(10)
γ [°]		81.7600(10)
Volume [Å^3]	4514.78(16)	1074.11(3)
Z, calculated density [Mg/m^3]	8, 1.973	2, 1.743
Absorption coefficient [mm^{-1}]	4.962	1.791
F(000)	2744	579
Crystal size [mm]	$0.20 \times 0.15 \times 0.08$	$0.32 \times 0.25 \times 0.20$
θ range for data collection [°]	3.66 to 69.54	2.03 to 27.48
Index ranges	$0 \le h \le 23$, $0 \le k \le 25$, $-17 \le l \le 13$	$-13 \le h \le 13$, $-13 \le k \le 12$, $-14 \le l \le 11$
Reflections collected/unique	4251/4251	7843/4879
Refinement method	full-matrix least squares on F^2	full-matrix least squares on F^2
Data/restraints/parameters	4251/25/416	4879/2/296
Goodness-of-fit on F^2	1.048	1.068
Final *R* indices [$I > 2\sigma(I)$] (R_1, wR_2)	0.0597, 0.1612	0.0451, 0.1225
R indices (all data) (R_1, wR_2)	0.0643, 0.1676	0.0620, 0.1358
Largest diff. peak and hole [e·Å^{-3}]	2.055 and –1.109	1.044 and –0.723

[a] GOOF = $\{\Sigma[w(F_o^2 - F_c^2)^2]/(n-p)\}^{1}/_{2}$, $R_1 = \Sigma||F_o| - |F_c||/\Sigma|F_o|$, $wR_2 = \{\Sigma[w(F_o^2 - F_c^2)^2]/\Sigma[w(F_o^2)^2]\}^{1}/_{2}$, $w = 1/[\sigma^2(F_o^2) + (aP)^2 + bP]$, where $P = [\max(F_o^2,0) + 2F_c^2]/3$; $a = 0.1163$, $b = 18.2879$ for **1** and $a = 0.0678$, $b = 2.2442$ for **2**.

Acknowledgments

Authors E. A., S. F., J. B., and M. L.-G. are grateful to MCyT (grant CTQ2004–03735/BQU), and authors H. R.-P. and S. G.-G. to MCyT (grant BQU2003–05093) and FICYT (grant PR-01-GE-4) for financial support.

[1] J. G. Haasnoot, *Coord. Chem. Rev.* **2000**, *200–202*, 131.
[2] a) M. H. Klingele, S. Brooker, *Coord. Chem. Rev.* **2003**, *241*, 119; b) U. Beckmann, S. Brooker, *Coord. Chem. Rev.* **2003**, *245*, 17.
[3] J. P. Zhang, Y.-Y. Lin, X.-C. Huang, X.-M. Chen, *J. Am. Chem. Soc.* **2005**, *127*, 5495.
[4] P. Gütlich, A. Hauser, H. Spiering, *Angew. Chem. Int. Ed. Engl.* **1994**, *33*, 2024.
[5] L. G. Lavrenova, S. V. Larionov, *Koord. Khim.* **1998**, *24*, 403.
[6] P. J. van Koningsbruggen, *Top. Curr. Chem.* **2004**, *233*, 123.
[7] M. Klingele, B. Moubaraki, J. D. Cashion, K. S. Murray, S. Brooker, *Chem. Commun.* **2005**, 987.
[8] A. C. Fabretti, *J. Crystallogr. Spectrosc. Res.* **1992**, *22*, 523.
[9] H. O. Desseyn, A. C. Fabretti, W. Malavasi, *J. Crystallogr. Spectrosc. Res.* **1990**, *20*, 355.
[10] A. C. Fabretti, A. Giusti, R. Sessoli, *Inorg. Chim. Acta* **1993**, *205*, 53.
[11] S. R. Grap, L. G. Kuz′mina, O. Y. Burtseva, M. A. Porai-Koshits, A. P. Kurbakova, I. A. Efimenko, *Zh. Neorg. Khim.* **1991**, *36*, 1427.
[12] S. R. Grap, L. G. Kuz′mina, M. A. Porai-Koshits, A. P. Kurbakova, I. A. Efimenko, *Koord. Khim.* **1993**, *19*, 566.
[13] L. Antolini, A. C. Fabretti, D. Gatesschi, A. Giusti, R. Sessoli, *Inorg. Chem.* **1991**, *30*, 4858.
[14] L. Antolini, A. C. Fabretti, D. Gatesschi, A. Giusti, R. Sessoli, *Inorg. Chem.* **1990**, *29*, 143.
[15] T. B. Brill, A. L. Rheingold, M. B. Allen, *Private Communication, CCD.* **1996**, NADHAB.
[16] Y. B. Brill, A. L. Rheingold, A. M. Allen, *Private Communication, CCD.* **1996**, NADPAJ.
[17] Recently, during the process of the revision of this manuscript, a 3D Cu^I–guanazole compound, synthesized under solvothermal conditions, has been structurally characterized: $[(H_3O)_2(H_2O)_4][\{Cu_6(datrz)_6\}\{(Cu_4I_4)_2O\}]$; see Q. G. Zhai, C.-Z. Lou, S.-M. Chen, X.-J. Xu, W.-B. Yang, *Inorg. Chem. Commun.* **2006**, *9*, 819.
[18] P. M. Slangen, P. J. van Koningsbruggen, K. Goubitz, J. G. Haasnoot, J. Reedijk, *Inorg. Chem.* **1994**, *33*, 1121.
[19] S. Ferrer, P. J. van Koningsbruggen, J. G. Haasnoot, J. Reedijk, H. Kooijman, A. L. Spek, L. Lezama, A. M. Arif, J. S. Miller, *J. Chem. Soc., Dalton Trans.* **1999**, 4269.
[20] L. Yi, B. Zhao, P. Cheng, D.-Z. Liao, S.-P. Yan, Z.-H. Jiang, *Inorg. Chem.* **2004**, *43*, 33.
[21] After submission of this manuscript, the authors were informed of three new dinuclear structures of Ni^{II} with one water and two triazole bridges: a) J.-H. Zhou, R.-M. Cheng, Y. Song, Y.-Z. Li, Z. Yu, X.-T. Chen, X.-Z. You, *Polyhedron* **2006**, *25*, 2426; b) P. Ren, B. Ding, W. Shi, Y. Wang, T. Lu, P. Cheng, *Inorg. Chim. Acta* **2006**, *359*, 3824.
[22] P. J. van Koningsbruggen, J. W. van Hal, R. A. G. de Graaff, J. G. Haasnoot, J. Reedijk, *J. Chem. Soc., Dalton Trans.* **1993**, 2163.
[23] S. F. Keij, Ph. D. Thesis, Leiden University, The Netherlands, **1990**.
[24] R. Prins, M. Biagini-Cingi, M. Drillon, R. A. G. de Graff, J. Haasnoot, A.-M. Manotti-Lanfredi, P. Rabu, J. Reedijk, F. Ugozzoli, *Inorg. Chim. Acta* **1996**, *248*, 35.
[25] J.-C. Liu, D.-G. Fu, J.-Z. Zhuang, C.-Y. Duan, X.-Z. You, *J. Chem. Soc., Dalton Trans.* **1999**, 2337.
[26] a) W. Vreugdenhil, J. G. Haasnoot, J. Reedijk, J. S. Wood, *Inorg. Chim. Acta* **1990**, *167*, 109; b) W. Vreugdenhil, Ph. D. Thesis, Leiden University, The Netherlands, **1987**.

[27] Y. Garcia, P. J. van Koningsbruggen, G. Bravic, P. Guionneau, D. Chasseau, G. L. Cascarano, J. Moscovici, K. Lambert, A. Michalowicz, O. Kahn, *Inorg. Chem.* **1997**, *36*, 6357.
[28] F. J. Rietmeijer, G. A. van Albada, R. A. G. de Graaff, J. G. Haasnoot, J. Reedijk, *Inorg. Chem.* **1985**, *24*, 3597.
[29] F. J. Rietmeijer, J. G. Haasnoot, A. J. Den Hartog, J. Reedijk, *Inorg. Chim. Acta* **1986**, *113*, 147.
[30] Q. Zhao, H. Li, A. Chen, R. Fang, *Inorg. Chim. Acta* **2002**, *336*, 142.
[31] G. A. van Albada, R. A. G. de Graaff, J. Haasnoot, J. Reedijk, *Inorg. Chem.* **1984**, *23*, 1404.
[32] J.-C. Liu, Y. Song, J.-Z. Zhuang, X.-Z. You, X.-Y. Huang, Z.-X, *Jiegou Huaxue* **2000**, *19*, 81.
[33] J.-C. Liu, Y. Xu, C.-Y. Duan, S.-L. Wang, F.-L. Liao, J.-Z. Zhuang, X.-Z. You, *Inorg. Chim. Acta* **1999**, *295*, 229.
[34] J. A. J. Jarvis, *Acta Crystallogr.* **1962**, *15*, 964.
[35] R. Prins, P. J. Birker, J. G. Haasnoot, G. C. Verschoor, J. Reedijk, *Inorg. Chem.* **1985**, *24*, 4128.
[36] W. M. E. Koomen-van-Oudenniel, R. A. G. de Graaff, J. G. Haasnoot, R. Prins, J. Reedijk, *Inorg. Chem.* **1989**, *28*, 1128.
[37] P. J. van Koningsbruggen, J. G. Haasnoot, R. A. G. de Graaff, J. Reedijk, S. Slingerland, *Acta Crystallogr., Sect. C: Cryst. Struct. Commun.* **1992**, *48*, 1923.
[38] P. M. Slangen, P. J. van Koningsbruggen, J. G. Haasnoot, J. Jansen, S. Gorter, J. Reedijk, H. Kooijman, W. J. J. Smeets, A. L. Spek, *Inorg. Chim. Acta* **1993**, *212*, 289.
[39] P. J. van Koningsbruggen, J. G. Haasnoot, H. Kooijman, J. Reedijk, A. L. Spek, *Inorg. Chem.* **1997**, *36*, 2487.
[40] O. Castillo, U. García-Couceiro, A. Luque, Juan P. García-Terán, P. Román, *Acta Crystallogr. Sect. E: Struct. Rep. Online* **2004**, *60*, m9-m11, DOI: 10.1107/S1600536803027119.
[41] M. H. Klingele, P. D. Boyd, B. Moubaraki, K. S. Murray, S. Brooker, *Eur. J. Inorg. Chem.* **2005**, 910.
[42] M. H. Klingele, P. D. Boyd, B. Moubaraki, K. S. Murray, S. Brooker, *Eur. J. Inorg. Chem.* **2006**, 573.
[43] For the first example of a structurally characterized triazolate-containing *macrocyclic* copper compound, see: C. V. Depree, U. Beckmann, K. Heslop, S. Brooker, *Dalton Trans.* **2003**, 3071.
[44] U. Beckmann, S. Brooker, C. V. Depree, J. D. Ewing, B. Moubaraki, K. S. Murray, *Dalton Trans.* **2003**, 1308.
[45] G. Vos, R. A. G. de Graaff, J. Haasnoot, A. M. van der Kraan, P. de Vaal, J. Reedjik, *Inorg. Chem.* **1984**, *23*, 2905.
[46] Y. Journaux, J. Sletten, O. Kahn, *Inorg. Chem.* **1986**, *25*, 439.
[47] R. Veit, J.-J. Girerd, O. Kahn, F. Robert, Y. Jeannin, *Inorg. Chem.* **1986**, *25*, 4175.
[48] O. Kahn, in *Magneto-Structural Correlations in Exchange Coupled Systems* (Eds.: D. Gatteschi, O. Kahn, R. D. Willet), NATO Advanced Study Institute Series, Reidel, Dordrecht, **1984**, vol. C140.
[49] V. K. Kumar, G. Keresztury, T. Sundius, R. J. Xavier, *Spectrochim. Acta, Part A* **2005**, *61*, 261.
[50] K. Nakamoto in *Infrared and Raman Spectra of Inorganic and Coordination Compounds: Part B: Applications in Coordination, Organometallic and Bioinorganic Chemistry*, 5th ed., John Wiley and Sons, New York, **1997**.
[51] B. J. Hathaway, D. E. Billing, *Coord. Chem. Rev.* **1970**, *5*, 143.
[52] J. Reedijk, D. Knetsch, B. Nieuwenhuisje, *Inorg. Chim. Acta* **1971**, *5*, 568.
[53] K. Nonoyama, H. Ojima, M. Nonoyama, *Inorg. Chim. Acta* **1984**, *84*, 13.
[54] J. R. Wasson, C.-I. Shyr, C. Trapp, *Inorg. Chem.* **1968**, *7*, 469.
[55] L. Banci, A. Bencini, D. Gatteschi, *Inorg. Chem.* **1983**, *22*, 2681.
[56] B. G. van den Bos, *Recl. Trav. Chim. Pays-Bas* **1960**, *79*, 836.
[57] Z. Otwinowski, W. Minor, *DENZO-SCALEPACK–Processing of X-ray Diffraction Data Collected in Oscillation Mode, Methods in Enzymology, Volume 276: Macromolecular Crystallography, Part A* (Eds.: C. W. Carter Jr., R. M. Sweet), Academic Press, New York, **1997**, pp. 307–326.
[58] *COLLECT*, Nonius BV, Delft, The Netherlands, **2000**.
[59] P. T. Beurskens, G. Beurskens, R. de Gelder, S. García-Granda, R. O. Gould, R. Israel, J. M. M. Smits, *The DIRDIF-99 Program System – Technical Report of the Crystallography Laboratory*, University of Nijmegen, The Netherlands, **1999**.
[60] *SIR97*: A. Altomare, M. C. Burla, M. Camalli, G. L. Cascarano, C. Giacovazzo, A. Guagliardi, A. G. G. Moliterni, G. Polidori, R. Spagna, *J. Appl. Crystallogr.* **1999**, *32*, 115.
[61] G. M. Sheldrick, *SHELX97–Programs for Crystal Structure Analysis* (Release 97–2), University of Göttingen, Germany, **1997**.
[62] *ORTEP3 for Windows*:L. J. Farrugia, *J. Appl. Crystallogr.* **1997**, *30*, 565.
[63] *International Tables for X-ray Crystallography* (Ed.: T. Hahn), Kluwer Academic Publishers, Dordrecht, The Netherlands, **1995**, vol. A.
[64] a) M. Nardelli, *Comput. Chem.* **1983**, *7*, 95; b) M. Nardelli, *Comput. Chem.* **1995**, *28*, 659.

Received: July 31, 2006
Published Online: November 3, 2006

